Bioorganic & Medicinal Chemistry Letters 25 (2015) 3910–3913

Contents lists available at ScienceDirect

Bioorganic & Medicinal Chemistry Letters

journal homepage: www.elsevier.com/locate/bmcl

Synthesis and inhibitory activity of substrate-analog fructosyl peptide oxidase inhibitors

Bunta Watanabe [a,*], Atsushi Ichiyanagi [b], Kozo Hirokawa [b], Keiko Gomi [b], Toru Nakatsu [c], Hiroaki Kato [c], Naoki Kajiyama [b]

[a] Institute for Chemical Research, Kyoto University, Gokasho, Uji, Kyoto 611-0011, Japan
[b] Research and Development Division, Kikkoman Corporation, 399 Noda, Noda, Chiba 278-0037, Japan
[c] Graduate School of Pharmaceutical Sciences, Kyoto University, 46-29 Yoshida-Shimo-Adachi-cho, Sakyo-ku, Kyoto 606-8501, Japan

ARTICLE INFO

Article history:
Received 4 May 2015
Revised 6 July 2015
Accepted 16 July 2015
Available online 23 July 2015

Keywords:
Diabetes
Glycation
Hemoglobin A1c
Fructosyl peptide oxidase
Substrate-analog inhibitor

ABSTRACT

Fructosyl peptide oxidases (FPOXs) play a crucial role in the diagnosis of diabetes. Their main function is to cleave fructosyl amino acids or fructosyl peptides into glucosone and the corresponding amino acids/dipeptides. In this study, the substrate-analog FPOX inhibitors **1a**–**c** were successfully designed and synthesized. These inhibitors mimic N^{α}-fructosyl-L-valine (Fru-Val), [N^{α}-fructosyl-L-valyl]-L-histidine (Fru-ValHis), and N^{ε}-fructosyl-L-lysine (εFru-Lys), respectively. The secondary nitrogen atom in the natural substrates, linking fructose and amino acid or dipeptide moieties, was substituted in **1a**–**c** with a sulfur atom to avoid enzymatic cleavage. Kinetic studies revealed that **1a**–**c** act as competitive inhibitors against an FPOX obtained from *Coniochaeta* sp., and K_i values of 11.1, 66.8, and 782 μM were obtained for **1a**–**c**, respectively.

Diabetes is a metabolic disorder, in which the patient suffers from chronically high concentrations of blood sugar. This condition inevitably leads to a high level of glycation, a non-enzymatic reduction between sugars such as glucose and free amino groups on amino acids or proteins. Clinically, the level of glycated hemoglobin (HbA1c) represents an important marker for the diagnosis of diabetes. Typically, the half-life of erythrocytes, a source of hemoglobin, is 110–120 days,[1] and the degree of glycation of hemoglobin can accordingly be used as a parameter to evaluate an average blood glucose concentration over the preceding weeks to months.[2] The quantification of HbA1c is therefore a good index for the therapeutic assessment and monitoring of diabetes patients. Today, a combination of enzymatic degradation of HbA1c and quantification of the resultant fructosyl peptides by fructosyl peptide oxidases (FPOXs)[3,4] is commonly used for the quantification of HbA1c. FPOXs oxidize fructosyl amino acids and peptides to Schiff bases, which can be hydrolyzed to generate glucosone and free amino acids and peptides (Scheme 1). The quantity of H_2O_2 liberated during the catalytic cycle of FPOXs thereby reflects the level of glycated proteins.

One of the major limitations of the enzymatic method described above is the degradation step of intact HbA1c. Even though FPOXs from *Coniochaeta* sp. (FPOX-C) and *Eupenicillium terrenum* (FPOX-E) are active toward fructosyl amino acids and a fructosyl dipeptide such as, for example, N^{α}-fructosyl-L-valine (Fru-Val), [N^{α}-fructosyl-L-valyl]-L-histidine (Fru-ValHis), and N^{ε}-fructosyl lysine (εFru-Lys), they are inactive toward fructosyl polypeptides. However, recent reports have described the reactivity of FPOX from *Phaeosphaeria nodorum* toward fructosyl hexapeptide.[5] This result encouraged us to use protein-engineering approaches to design and develop novel FPOXs that are able to interact with HbA1c. For such manipulations, detailed information about the precise three-dimensional structure and substrate recognition mechanism of the parent enzymes are indispensible. Recently, preliminary results of the crystallographic analysis of FPOXs were reported by us[6] and other research groups.[7] However, as the crystals employed in these studies did not contain any ligands, the substrate recognition mechanism still remains elusive. The generation of FPOX inhibitors for the co-crystallization with proteins therefore represents

Abbreviations: HbA1c, hemoglobin A1c; FPOX, fructosyl peptide oxidase; FAD, flavin adenine dinucleotide; CFP-T7, thermostable fructosyl peptide oxidase mutant; rt, room temperature; quant, quantitative; aq, aqueous; Tf, trifluoromethanesulfonyl; Trt, triphenylmethyl; COMU, *N*-[1-(cyano-2-ethoxy-2-oxoethylideneaminooxy)dimethylamino(morpholino)]uronium hexafluorophosphate; Boc, *tert*-butoxycarbonyl; DMAP, 4-(dimethylamino)pyridine; BzSCs, cesium thiobenzoate; RPLC, reverse-phase liquid chromatography; TFA, trifluoroacetic acid.

* Corresponding author. Tel.: +81 774 38 3233; fax: +81 774 38 3229.
E-mail address: bunta@scl.kyoto-u.ac.jp (B. Watanabe).

http://dx.doi.org/10.1016/j.bmcl.2015.07.045
0960-894X/

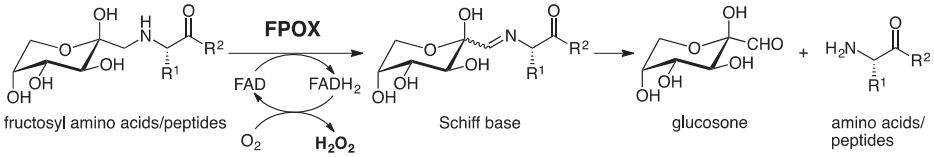

Scheme 1. FPOX-catalyzed reactions.

a highly desirable research target. Due to their structural similarity to substrates, substrate-analog inhibitors should be accommodated on the active site of the enzyme but display tolerance toward enzymatic transformation. In order to successfully design such inhibitors, minimal structural changes that retain the binding affinity to target the enzyme are important.

In this study, we designed and synthesized the novel substrate-analog FPOX inhibitors **1a**–**c** (Fig. 1), which allowed us to unveil the precise structure and the substrate recognition mechanism of FPOXs. As shown in Figure 1, **1a**–**c** are analogs of Fru-Val, Fru-ValHis, and εFru-Lys, respectively. We substituted the nitrogen atom in the natural FPOX substrates (Fru-Val, Fru-ValHis, and εFru-Lys) with a sulfur atom, as we assumed that this modification should avoid a significant loss of binding affinity of **1a**–**c** toward FPOX while simultaneously preventing the enzymatically-induced oxidative cleavage described in Scheme 1. A similar approach was successfully employed for the development of monomeric sarcosine oxidase and fructosamine oxidase inhibitors.[8,9] We also determined the inhibitory activity and the inhibition mechanism of **1a**–**c** against the thermostable FPOX-C mutant CFP-T7.[10]

The synthesis of the inhibitor **1a** is outlined in Scheme 2. Commercially available (*R*)-(+)-2-bromo-3-methylbutyric acid (**2**) was treated with cesium thiobenzoate (BzSCs), before the resulting thiobenzoate **3** was hydrolyzed to afford (*S*)-2-sulfanyl-3-methylbutanoic acid (**4**) in quantitative yield.[11,12] Introduction of a fructose moiety was achieved by a coupling reaction between thiol **4** and triflate **5**,[13] furnishing protected Fru-Val analog **6** in 72% yield.

As illustrated in Scheme 2, the acetonide-protected pyranose rings of **5** and **6** adopted a twisted-boat conformation in $CDCl_3$. This is reflected in the ^1H NMR coupling constants between the 3α-H and 4β-H (J = 2.4–2.8 Hz), which are considerably smaller than typical 1,2-diaxial coupling constants for a chair conformation (J = 8–10 Hz). In contrast, the coupling constants between 4β-H and 5β-H (J = 7.9 Hz) are considerably larger compared to typical 1,2-diequatorial coupling constants (J = 2–3 Hz); an observation that is consistent with a report by Maryanoff and co-workers.[14] Acidic hydrolysis of **6** resulted in the formation of Fru-Val analog inhibitor **1a**[15] in 59% yield after purification by reversed-phase liquid chromatography (RPLC). The ^1H NMR spectrum of **1a** in D_2O revealed that the sugar moiety adopted predominantly the β-

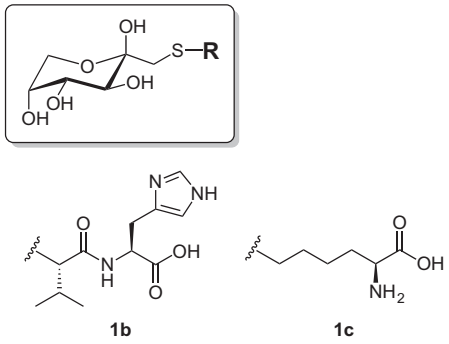

Figure 1. Chemical structures of FPOX inhibitors **1a**–**c**.

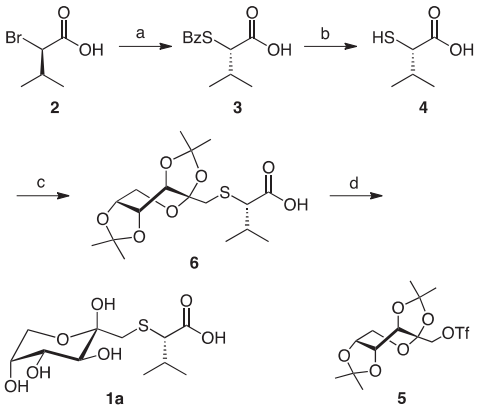

Scheme 2. Synthesis of inhibitor **1a**. Reagents and conditions: (a) BzSCs, DMF, rt, 2 d; (b) 5 M NH_3 aq, CH_2Cl_2, rt, 3 h, quant from **2**; (c) **5**, 1 M KOH aq, acetone, THF, reflux, 3 d, 72%; (d) TFA, H_2O, rt, 1.5 h, 59%.

pyranose form (ca. 75%). Coupling constants of 9.9 and 3.3 Hz were measured for 3α-H/4β-H and 4β-H/5β-H, respectively. These values suggest a 1,2-diaxial coupling between 3α-H and 4β-H, and a 1,2-diequatorial coupling between 4β-H and 5β-H. Accordingly, a chair conformation as shown in Scheme 2 was assigned to the pyranose ring of inhibitor **1a**.

The synthesis of inhibitor **1b** is outlined in Scheme 3. Compound **6** was coupled with the protected histidine derivative [H-His(Trt)-OMe·HCl] to afford **7**. A hydrolysis of the methyl ester group under basic conditions, followed by acidic hydrolysis of the acetonide and triphenylmethyl moieties furnished Fru-ValHis analog inhibitor **1b**[16] in 67% yield as the trifluoroacetic acid (TFA) free form after purification by RPLC. The pyranose rings of **7** and **1b** adopted twisted-boat and chair conformations, respectively.

Subsequently, a protected lysine counterpart was prepared for the synthesis of εFru-Lys analog inhibitor **1c** (Scheme 4). For that purpose, a combined one-pot protection procedure, using commercially available L-2-aminoadipic acid (**8**), was applied to the carboxy and amino groups,[17] resulting in the quantitative formation of mono-Boc derivative **9**. The mono-Boc amino group of **9** was

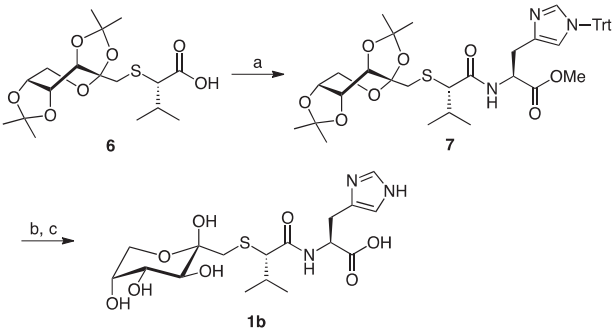

Scheme 3. Synthesis of inhibitor **1b**. Reagents and conditions: (a) [H-His(Trt)-OMe·HCl], COMU, 2,4,6-trimethylpyridine, DMF, rt, 2 h, 76%; (b) 0.5 M NaOH aq, MeOH, rt, 30 min; (c) TFA, H_2O, rt, 1 h, 67% from **7**.

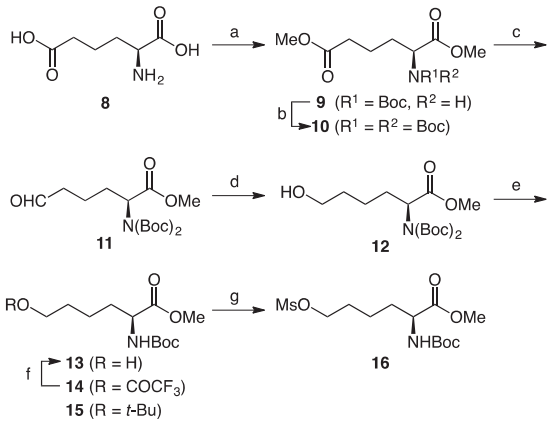

Scheme 4. Preparation of protected lysine counterpart **16**. Reagents and conditions: (a) (i) TMSCl, MeOH, rt, 2 d, (ii) $(Boc)_2O$, Et_3N, rt, 27 h, quant; (b) $(Boc)_2O$, DMAP, MeCN, 4 d, 95%; (c) $(i\text{-}Bu)_2AlH$, Et_2O, hexane, −78 °C, 15 min, 66%; (d) $NaBH_4$, MeOH, 0 °C, 20 min, 94%; (e) TFA, CH_2Cl_2, rt, 5 h, 60% (**13**), 22% + 11% (**14** + **15**); (f) $NaHCO_3$ aq, MeOH, rt, 30 min, 95%; (g) MsCl, Et_3N, CH_2Cl_2, rt, 1 h, quant.

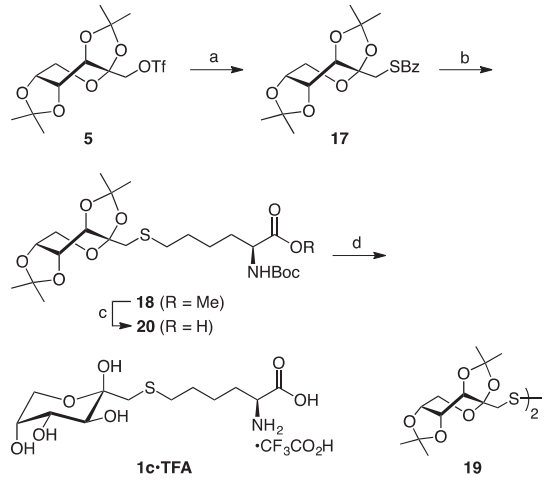

Scheme 5. Synthesis of inhibitor **1c**. Reagents and conditions: (a) BzSCs, DMF, rt, 17 h, 93%; (b) (i) NaOMe, MeOH, rt, 90 min, (ii) **16**, rt, 2 h, 96%; (c) 2.5 M NaOH aq, MeOH, rt, 1 h, 93%; (d) TFA, H_2O, rt, 30 min, 49%.

further protected to afford di-Boc derivative **10** in almost quantitative yield. The esterified carboxy group at the ω-end of **10** was selectively reduced with $(i\text{-}Bu)_2AlH$,[17] affording aldehyde **11** in 66% yield. After the reduction of the formyl group in **11**, the di-Boc protection of alcohol **12** was partially removed with TFA in CH_2Cl_2[18] to furnish mono-Boc alcohol **13**.[19] The moderate yield of the reaction (60%) should most likely be ascribed to the formation of a mixture of the esterified and etherified by-products **14** and **15**. Based on the ^1H NMR analysis of the mixture, the yields of **14** and **15** were estimated to be 22% and 11%, respectively. We made no attempt to separate this mixture, since hydrolysis under mildly basic conditions converted trifluoroacetate **14** into the more polar alcohol **13**, which allowed us to separate **13** and less polar **15** very easily. The yield of **13** thus obtained from **14** was 95%, and pure *t*-Bu ether **15** was recovered in 87% yield. A subsequent reaction of **13** with methanesulufonyl chloride furnished the protected lysine counterpart **16**[20] in quantitative yield.

The synthesis of inhibitor **1c** is shown in Scheme 5. Triflate **5** was treated with BzSCs to give thiobenzoate **17** in 93% yield. The benzoyl group of **17** was hydrolyzed with NaOMe, and the resulting thiolate anion was not isolated, but treated with mesylate **16** to afford the fully protected intermediate **18** in almost quantitative yield. It should be noted here, that these reaction conditions suppress the formation of the oxidative homocoupling by-product, namely disulfide **19**,[21] which was only observed in negligible amounts. The protecting groups of compound **18** were removed by consecutive basic and acidic hydrolysis. After purification by RPLC, εFru-Lys analog inhibitor **1c**[22] was obtained in 49% yield as the TFA salt.

The inhibitory activity of **1a**–**c** against CFP-T7 was monitored by a peroxidase-coupled reaction system. The details of the assay are described in the supporting information. Under the conditions applied, the Michaelis constants (K_m) of CFP-T7 were determined to be 0.940 ± 0.025, 0.513 ± 0.014, and 25.3 ± 0.5 mM for Fru-Val, Fru-ValHis, and εFru-Lys, respectively.[23] Accordingly, Fru-ValHis was selected as the substrate for the subsequent enzyme inhibition assay. Figure 2 shows the Lineweaver–Burk plots for **1a**–**c**, which clearly demonstrate that these act as competitive inhibitors, and inhibition constants (K_i) of 11.1 ± 0.9 (**1a**), 66.8 ± 0.8 (**1b**), and 782 ± 8 μM (**1c**) were obtained from Dixon plots.[23] These results indicate that the affinity of inhibitors **1a** and **1b** toward CFP-T7 is about 46 and 7.7 times greater than that of Fru-ValHis, the best substrate for the enzyme. Even though the affinity of εFru-Lys analog inhibitor **1c** for CFP-T7 is only 66% of that of Fru-ValHis, it is at least 30 times higher than that of the parent εFru-Lys, when considering that the K_m value of εFru-Lys (25.3 mM) is nearly 50 times higher than that of Fru-ValHis (0.513 mM).

The difference of inhibitory activity toward CFP-T7 between **1a**-**c** (K_i: 11.1–782 μM) was higher than that of affinity between the natural substrates (K_m: 0.940–25.3 mM). This should be attributed to the presence of the secondary amino group in the natural substrates. Possible formation of hydrogen bonds between the amino group and the surrounding residue(s) of CFP-T7 should constrain the substituent at C-1 position of the fructose ring more tightly.

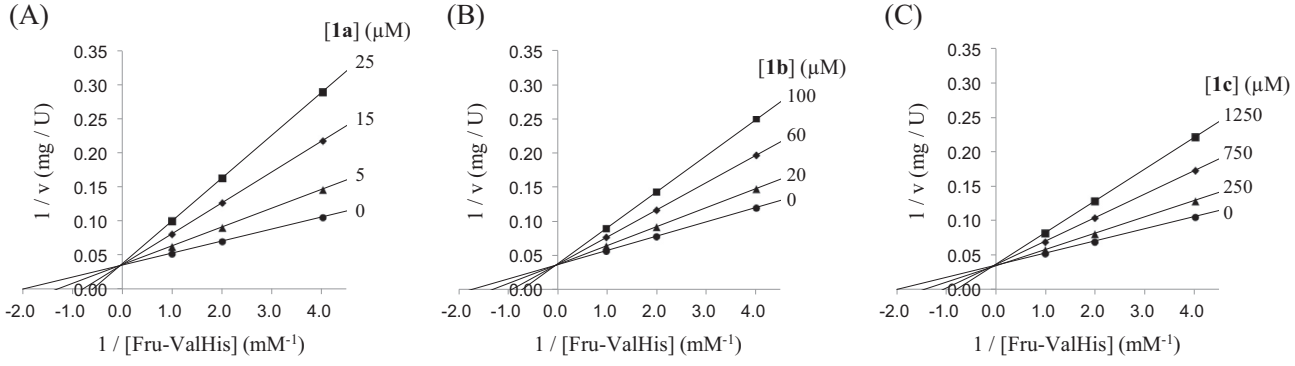

Figure 2. Lineweaver–Burk plots for various concentrations of the inhibitors **1a** (A), **1b** (B), and **1c** (C).

Since the inhibitors used in this study are unable to form such hydrogen bonds with CFP-T7, the corresponding inhibitor moiety seems to exhibit more degrees of freedom relative to the amino acid/dipeptide moiety of the natural compounds. The latitude of the inhibitors should be a drawback for the binding affinity toward the enzyme, and sterically less demanding substituents should be preferable. This effect probably affects the inhibitory activity of **1a-c** toward CFP-T7 strongly, and the inhibitory activity of Fru-Val analog **1a**, which contains the smallest substituent at the C-1 position of the fructose ring, was higher than that of Fru-ValHis analog **1b**. Regardless, natural Fru-ValHis proved to be the best substrate for CFP-T7.

In conclusion, we successfully designed and synthesized substrate-analog inhibitors for CFP-T7 and quantitatively analyzed their inhibition properties. Co-crystallization of the enzyme with inhibitors **1a**–**c** in order to determine the three-dimensional structure of CFP-T7 by X-ray crystallography is currently undertaken in our laboratories and results will be disseminated in due course.

Acknowledgements

Parts of the experimental measurements were carried out using the Bruker and JEOL 600 MHz NMR spectrometers, as well as the JOEL JMS-700 mass spectrometer in the Joint Usage/Research Center (JURC) at the Institute for Chemical Research, Kyoto University.

Supplementary data

Supplementary data associated with this article can be found, in the online version, at http://dx.doi.org/10.1016/j.bmcl.2015.07.045.

References and notes

1. Schultze, H. E.; Heremans, J. F. *Molecular Biology of Human Proteins*; Elsevier: Amsterdam, 1966. Vol. 1, Chapter 2.
2. Bunn, H. F.; Gabbay, K. H.; Gallop, P. M. *Science* **1978**, *200*, 21.
3. Hirokawa, K.; Gomi, K.; Kajiyama, N. *Biochem. Biophys. Res. Commun.* **2003**, *311*, 104.
4. Kim, S.; Ferri, S.; Tsugawa, W.; Mori, K.; Sode, K. *Biotechnol. Bioeng.* **2010**, *106*, 358.
5. Ferri, S.; Miyamoto, Y.; Sakaguchi-Mikami, A.; Tsugawa, W.; Sode, K. *Mol. Biotechnol.* **2013**, *54*, 939.
6. Ichiyanagi, A.; Hirokawa, K.; Gomi, K.; Nakatsu, T.; Kato, H.; Kajiyama, N. *Acta Crystallogr., Sect. F* **2013**, *69*, 130.
7. Xing, K.; Gan, W.; Jia, M.; Gao, F.; Gong, W. *Acta Crystallogr., Sect. F* **2013**, *69*, 666.
8. Wagner, M. A.; Trickey, P.; Chen, Z. W.; Mathews, F. S.; Jorns, M. S. *Biochemistry* **2000**, *39*, 8813.
9. Collard, F.; Zhang, J.; Nemet, I.; Qanungo, K. R.; Monnier, V. M.; Yee, V. C. *J. Biol. Chem.* **2008**, *283*, 27007.
10. Hirokawa, K.; Ichiyanagi, A.; Kajiyama, N. *Appl. Microbiol. Biotechnol.* **2008**, *78*, 775.
11. Strijtveen, B.; Kellogg, R. M. *J. Org. Chem.* **1986**, *51*, 3664.
12. Perrine, S. P. US2008/0075692.
13. Maryanoff, B. E.; McComsey, D. F.; Costanzo, M. J.; Hochman, C.; Smith-Swintosky, V.; Shank, R. P. *J. Med. Chem.* **1941**, *2005*, 48.
14. Maryanoff, B. E.; Nortey, Samuel O.; Gardocki, J. F.; Shank, R. P.; Dodgson, S. P. *J. Med. Chem.* **1987**, *30*, 880.
15. Compound **1a**: colorless, hygroscopic solid. ^{1}H NMR (600 MHz, D_2O) δ_H: 1.02 (3H, d, J = 6.8 Hz, Val-γH_3-2), 1.07 (3H, d, J = 6.8 Hz, Val-γH_3-1), 1.99–2.07 (1H, m, Val-βH), 2.95 (1H, d, J = 14.1 Hz, Fru-1H_a), 3.01 (1H, d, J = 14.1 Hz, Fru-1H_b), 3.35 (1H, d, J = 8.4 Hz, Val-αH), 3.65 (1H, dd, J = 12.9, 1.3 Hz, Fru-6H_a), 3.82 (1H, d, J = 9.9 Hz, Fru-3H), 3.85 (1H, dd, J = 9.9, 3.3 Hz, Fru-4H), 3.96–3.99 (1H, m, Fru-5H), 3.97 (1H, dd, J = 12.9, 1.3 Hz, Fru-6H_b). ^{13}C NMR (151 MHz, D_2O) δ_C: 22.07 (Val-γ-1), 22.58 (Val-γ-2), 32.94 (Val-β), 41.40 (Fru-1), 59.17 (Val-α), 66.26 (Fru-6), 71.92 (Fru-5), 72.26 (Fru-3), 72.56 (Fru-4), 101.40 (Fru-2), 180.24 (Val-carbonyl). HRMS-FAB (m/z): $[M+Na]^+$ calcd. for $C_{11}H_{20}NaO_7S$: 319.0827; found: 319.0826.
16. Compound **1b**: colorless solid. ^{1}H NMR (600 MHz, D_2O) δ_H: 0.90 (3H, d, J = 6.7 Hz, Val-γH_3-1), 1.01 (3H, d, J = 6.7 Hz, Val-γH_3-2), 1.87–1.97 (1H, m, Val-β), 2.69 (1H, d, J = 13.8 Hz, Fru-1H_a), 2.83 (1H, d, J = 13.8 Hz, Fru-1H_b), 3.13 (1H, dd, J = 15.6, 9.3 Hz, His-βH_a), 3.30 (1H, d, J = 8.9 Hz, Val-αH), 3.32 (1H, ddd, J = 15.6, 5.0, 1.0 Hz, His-βH_b), 3.66 (1H, dd, J = 12.8, 1.8 Hz, Fru-6H_a), 3.72 (1H, d, J = 9.9 Hz, Fru-3H), 3.86 (1H, dd, J = 9.9, 3.5 Hz, Fru-4H), 3.97 (1H, dd, J = 12.8, 1.3 Hz, Fru-6H_b), 3.98–3.99 (1H, m, Fru-5H), 4.60 (1H, dd, J = 9.3, 5.0 Hz, His-αH), 7.338–7.340 (1H, m, His-Im-5H), 8.63 (1H, d, J = 1.4 Hz, His-Im-2H). ^{13}C NMR (151 MHz, D_2O) δ_C: 22.32 (Val-γ-1), 22.65 (Val-γ-2), 30.02 (His-β), 33.36 (Val-β), 41.06 (Fru-1), 56.55 (His-α), 59.98 (Val-α), 66.32 (Fru-6), 71.85 (Fru-5), 72.54 (Fru-4), 72.67 (Fru-3), 101.31 (Fru-2), 119.76 (His-Im-5), 132.40 (His-Im-4), 136.11 (His-Im-2), 177.39 (Val-carbonyl), 178.68 (His-carbonyl). HRMS-FAB (m/z): $[M+H]^+$ calcd. for $C_{17}H_{28}N_3O_8S$: 434.1597; found: 434.1594.
17. Padrón, J. M.; Kokotos, G.; Martín, T.; Markidis, T.; Gibbons, W. A.; Martín, V. S. *Tetrahedron: Asymmetry* **1998**, *9*, 3381.
18. Koseki, Y.; Yamada, H.; Usuki, T. *Tetrahedron: Asymmetry* **2011**, *22*, 580.
19. Compound **13** has previously been synthesized via an independent route; see: Rodriguez, A.; Miller, D. D.; Jackson, R. F. W. *Org. Biomol. Chem.* **2003**, *1*, 973.
20. Compound **16** has been previously synthesized by an independent route, but NMR and MS data were not reported; see: Fanning, K. N.; Sutherland, A. *Tetrahedron Lett.* **2007**, *48*, 8479.
21. Goodwin, J. C. *Carbohydr. Res.* **1989**, *195*, 150.
22. Compound **1c**: pale yellow, hygroscopic solid. ^{1}H NMR (600 MHz, D_2O) δ_H: 1.45–1.58 (2H, m, Lys-γH_2), 1.66 (2H, dddd, J = 7.3 Hz each, Lys-δH_2), 1.89–2.02 (2H, m, Lys-βH_2), 2.65 (1H, dt, J = 12.9, 7.3 Hz, Lys-εH_a), 2.68 (1H, dt, J = 12.9, 7.3 Hz, Lys-εH_b), 2.91 (1H, d, J = 14.0 Hz, Fru-1H_a), 2.94 (1H, d, J = 14.0 Hz, Fru-1H_b), 3.64 (1H, dd, J = 12.9, 2.1 Hz, Fru-6H_a), 3.80 (1H, d, J = 10.0 Hz, Fru-3H), 3.86 (1H, dd, J = 10.0, 3.4 Hz, Fru-4H), 3.96–3.98 (1H, m, Fru-5H), 3.97 (1H, dd, J = 12.9, 1.4 Hz, Fru-6H_b), 4.06 (1H, dd, J = 7.0, 5.6 Hz, Lys-αH). ^{13}C NMR (151 MHz, D_2O) δ_C: 25.98 (Lys-γ), 30.97 (Lys-δ), 32.08 (Lys-β), 35.15 (Lys-ε), 41.61 (Fru-1), 55.68 (Lys-α), 66.32 (Fru-6), 71.87 (Fru-5), 72.45 (Fru-3), 72.56 (Fru-4), 101.50 (Fru-2), 119.16 (q, J_{C-F} = 291 Hz, TFA-CF_3), 165.79 (q, J_{C-F} = 35.6 Hz, TFA-carbonyl), 175.11 (Lys-carbonyl). ^{19}F NMR (565 MHz, D_2O) δ_F: −75.5. HRMS-FAB (m/z): $[M-TFA+H]^+$ calcd. for $C_{12}H_{24}NO_7S$: 326.1273; found: 326.1275.
23. Data given represent the mean results ± standard deviations from three independent experiments.